Cell, Vol. 100, 221–228, January 21, 2000, Copyright ©2000 by Cell Press

Phosphatidylinositol 4,5-Bisphosphate Functions as a Second Messenger that Regulates Cytoskeleton–Plasma Membrane Adhesion

Drazen Raucher,* Thomas Stauffer,* Wen Chen,* Kang Shen,* Shuling Guo,† John D. York,† Michael P. Sheetz,* and Tobias Meyer*†‡
*Department of Cell Biology
†Department of Pharmacology and Cancer Biology
Duke University Medical Center
Durham, North Carolina 27710

Summary

Binding interactions between the plasma membrane and the cytoskeleton define cell functions such as cell shape, formation of cell processes, cell movement, and endocytosis. Here we use optical tweezers tether force measurements and show that plasma membrane phosphatidylinositol 4,5-bisphosphate (PIP2) acts as a second messenger that regulates the adhesion energy between the cytoskeleton and the plasma membrane. Receptor stimuli that hydrolyze PIP2 lowered adhesion energy, a process that could be mimicked by expressing PH domains that sequester PIP2 or by targeting a 5′-PIP2-phosphatase to the plasma membrane to selectively lower plasma membrane PIP2 concentration. Our study suggests that plasma membrane PIP2 controls dynamic membrane functions and cell shape by locally increasing and decreasing the adhesion between the actin-based cortical cytoskeleton and the plasma membrane.

Introduction

The plasma membrane (PM) of cells conforms to the shape of the cortical cytoskeleton, suggesting that significant adhesive interactions exist between the plasma membrane and the cytoskeleton. The regulation of this cytoskeleton-membrane adhesion energy is of fundamental importance not only for the overall cell shape but also in the regulation of a variety of cell functions. Particularly, cytoskeletal–membrane interactions drive the formation and retraction of filopodia, lamellipodia, neurites, and other membrane processes in response to chemoattractants and other stimuli. Cytoskeletal–membrane interactions are also thought to regulate the rates of exocytosis and endocytosis and to control signaling processes.

While extracellular membrane adhesion to substrates has been intensely studied and is well understood, less is known about the molecular mechanisms that regulate intracellular adhesion between the cytoskeletal and plasma membrane. The overall interaction appears to be complex since many cytoskeletal proteins have been identified that bind to integral membrane proteins as well as to membrane phospholipids. Nevertheless, the combined dynamic interaction between different cytoskeleton and plasma membrane components can be described by a simple energy term that can be measured by separating the plasma membrane from the underlying cytoskeleton using optical tweezers or other methods (Waugh and Bauserman, 1995; Hochmuth et al., 1996; Raucher and Sheetz, 1999). By understanding the mechanisms that regulate the cytoskeletal–membrane adhesion energy, one can gain insights into cell functions such as formation of membrane processes, cell movement, signaling, and endocytosis.

How is the membrane–cytoskeletal adhesion energy regulated? Plasma membrane phosphatidylinositol 4,5-bisphosphate (PIP2) is an interesting candidate for such a master regulator since it can directly bind to many cytoskeletal proteins and since it also serves as a precursor for the second messengers PIP3, calcium, and diacylglycerol, which may act in parallel with PIP2 in regulating cytoskeletal structure. Here we investigate the link between PIP2 and cytoskeletal–membrane adhesion energy by manipulating plasma membrane PIP2 concentrations and by measuring adhesion energy using tether force measurements with optical tweezers.

Results and Discussion

Expression of a PIP2-Specific PH Domain Decreases Cytoskeletal–Plasma Membrane Adhesion

The PIP2 dependence of the interactions between the plasma membrane and the cytoskeleton (Janmey, 1995; Kandzari et al., 1996; Ren and Schwartz, 1998) was investigated by pulling membrane tethers using optical tweezers (Dai and Sheetz, 1995; Raucher and Sheetz, 1999). One micrometer–diameter polystyrene beads coated with IgG were used to pull a thin membrane tether from NIH-3T3 fibroblasts (Figure 1A) (Kuo and Sheetz, 1993). At a constant length, the force on the bead was measured by its displacement from the center of the laser trap (Figures 1B and 1C). This tether force (F) is a measure of the apparent membrane tension or the energy required to move membrane from the plasma membrane into the tether. In a first approximation, it is proportional to the square root of the cytoskeleton–plasma membrane adhesion energy (γ) (see Experimental Procedures). This simple relationship between tether force and adhesion energy is based on the findings that tethers lack cytoskeletal support (Berk and Hochmuth, 1992; Waugh and Bauserman, 1995). We further tested for the presence of F-actin in tethers by comparing tethers costained with the membrane marker FM1-43 (Figure 1D, left) and with rhodamine phalloidin (Figure 1D, right). No F-actin staining could be observed. Tethers also retracted rapidly when the trap was turned off ($<$100 ms; data not shown), suggesting that these tethers have the same viscous properties as tethers pulled from lipid vesicles without cytoskeleton (Waugh and Bauserman, 1995). In resting fibroblasts, the measured tether force of 7 pN corresponds to a cytoskeleton-to-plasma membrane adhesion energy of approximately 9.1 10^{-18} J/μm^2

‡To whom correspondence should be addressed at the following present address: Department of Molecular Pharmacology, Stanford University School of Medicine, Stanford, California 94305 (e-mail: t.meyer@cellbio.duke.edu).

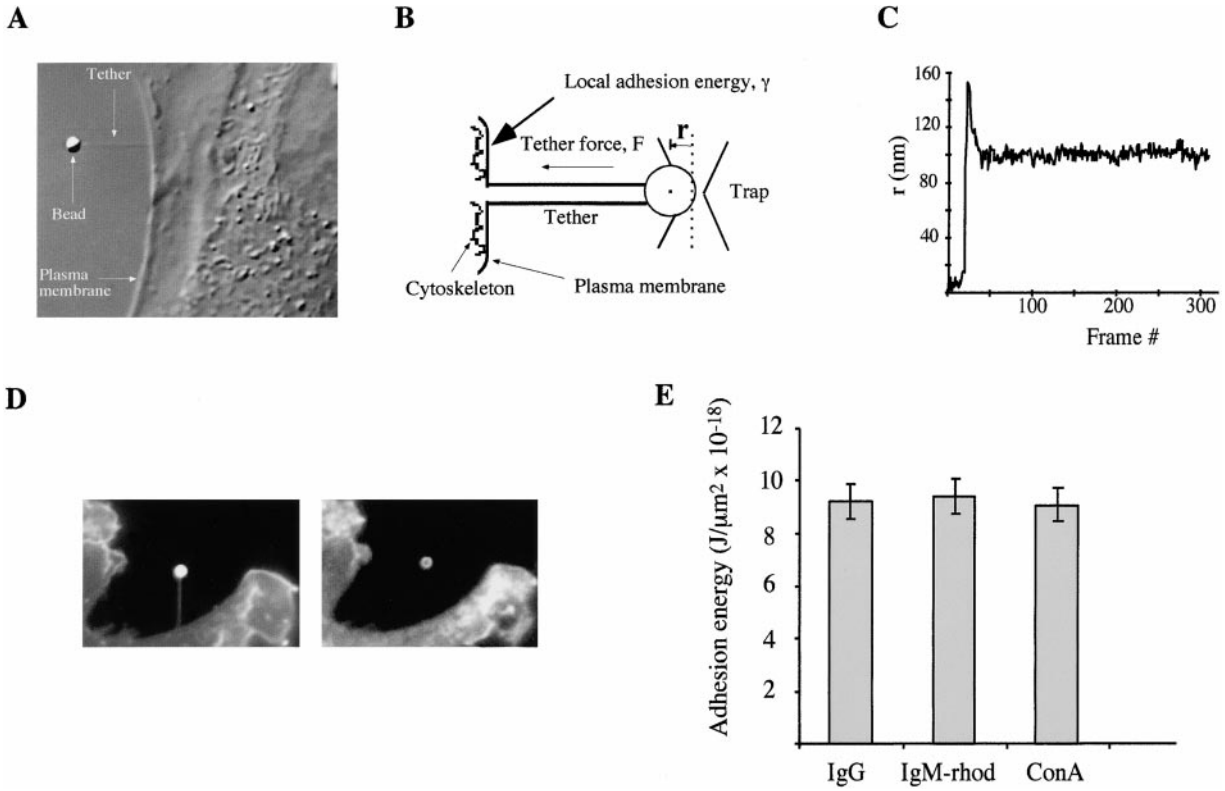

Figure 1. Tether Force Measurements of the Adhesion Energy between the Plasma Membrane and the Cortical Cytoskeleton

(A) DIC image of a tether force measurement using optical tweezers.

(B) Schematic view of the optical tweezers force measurement that defines the local adhesion energy term.

(C) Typical displacement trace, showing how far the center of the bead has been moved away from the center of the optical tweezers.

(D) The absence of F-actin in membrane tethers. A membrane marker FM1-43 staining of plasma membrane (left panel) and rhodamine phalloidin staining of F-actin (right panel).

(E) The measured adhesion energy is independent of the mechanism of bead attachment.

(see Experimental Procedures). This measured adhesion energy was not dependent on whether beads were coated with either IgG, IgM, or ConA (Figure 1E). Similarly, fibroblasts plated on glass, laminin, or polylysine had the same plasma membrane to cytoskeleton adhesion energy (data not shown).

We investigated the cellular roles of PIP2 by expressing pleckstrin homology (PH) domains that specifically sequester PIP2 (Stauffer et al., 1998). From several PIP2-binding PH domains that we tested (PH domains from PLCγ, PLCδ, and pleckstrin; data not shown), the green fluorescent protein (GFP)–tagged PH domain from phospholipase C δ (PLCδ) showed the highest ratio of plasma membrane to cytosolic localized GFP-PH (Figure 2A). This suggests that the PH domain from PLCδ has a high in vivo binding affinity for plasma membrane PIP2. As expected, a control construct with Lys30Asn and Lys32Asn mutations (GFP-PH*) that prevented PIP2-binding in vitro showed no plasma membrane localization (Figure 2B).

Expression of the PIP2-sequestering GFP-PH(PLCδ) construct dramatically reduced the adhesion energy (Figure 2C). In control measurements, the adhesion energy was the same in cells expressing GFP or GFP-PH*(PLCδ). Furthermore, the reduction in adhesion energy was specific for $PI(4,5)P_2$ over $PI(3,4)P_2$, since a GFP-PH(Akt) domain, which binds $PI(3,4)P_2$, had no effect (Franke et al., 1997; Isakoff et al., 1998). Since PH domain expression may change levels of PIP2, this may consequently alter baseline calcium or DAG concentrations. Therefore, we tested the effect of calcium and DAG on adhesion energy. Addition of phorbolester, diacylglycerol (DiC8), thapsigargin, and a combination of phorbolester and thapsigargin showed only a small reduction in adhesion energy. This suggests that the marked reduction in adhesion energy by PH(PLCδ) does not result from a change in the baseline DAG or calcium concentration (Figure 2C) but rather from a reduction of available PIP2.

Expression of Plasma Membrane Targeted 5′-Specific PIP2 Phosphatase Decreases Adhesion Energy

While the experiments with the expressed PH domain show that sequestration of plasma membrane PIP2 lipids by GFP-PH(PLCδ) lowers adhesion energy, we tested the connection between PIP2 concentration and adhesion energy more directly by using an enzymatic approach. Our strategy was to target a PIP2-specific 5′-phosphatase to the plasma membrane to selectively reduce plasma membrane PIP2 concentration but not other intracellular pools of PIP2 or other plasma membrane phosphatidylinositol phosphates (Figure 3A). We achieved

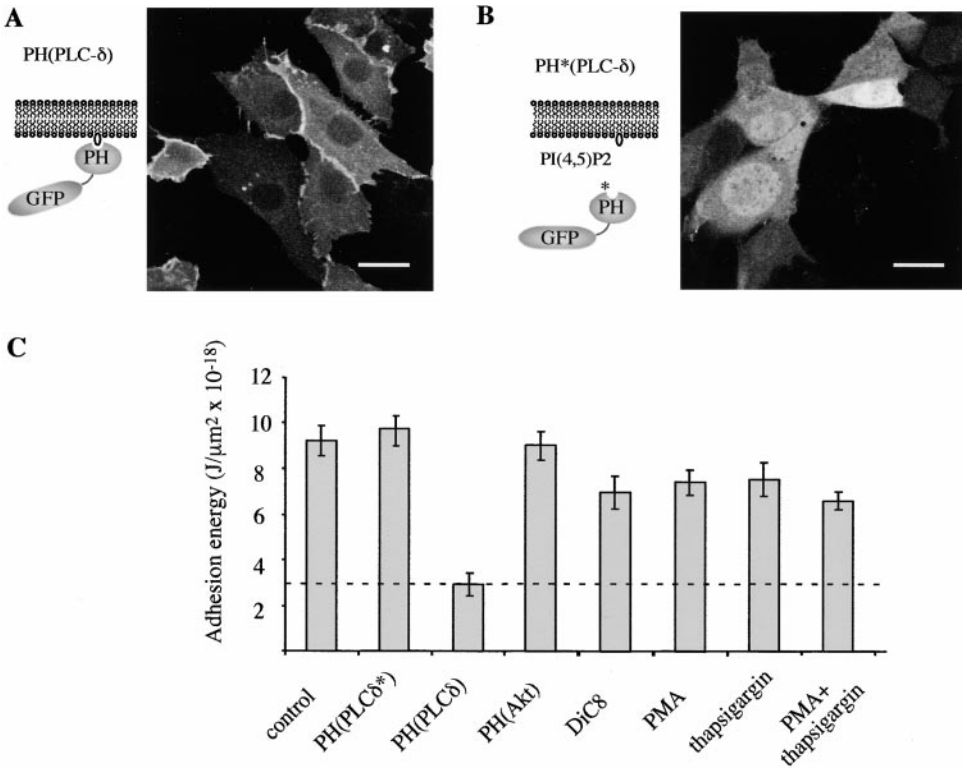

Figure 2. Expression of PH Domains that Selectively Bind PI(4,5)P_2 Markedly Reduces Cytoskeletal–Plasma Membrane Adhesion Energy

(A) Schematic representation of the GFP–PH domain construct from PLCδ, GFP-PH(PLCδ), and its plasma membrane localization in NIH-3T3 cells.

(B) Cytosolic expression of a mutant control construct, GFP-PH*(PLCδ), which is deficient in PIP2 binding.

(C) Bar diagram of the adhesion energy in untransfected cells, in cells transfected with a mutant GFP-PH*(PLCδ) control construct, with GFP-PH(PLCδ), and with a GFP-tagged PH domain from Akt that binds PI(3,4)P_2. As an additional control, the changes in adhesion energy after a 10 min incubation with the PKC activators phorbolester (PMA, 100 nM) and DiC8 (10 μg/ml) are shown. Addition of thapsigargin (increases cytosolic calcium by blocking calcium store calcium pumps; 0.3 μM) and thapsigargin plus PMA (0.3 μM and 1 μM, respectively) also showed only a small effect on adhesion energy.

this goal by fusing a myristoylation/palmitoylation sequence as well as a GFP tag to Inp54p, a specific 5′-phosphatase (Stolz et al., 1998). The plasma membrane–localized expression of this construct is shown in Figure 3B (PM-5′-phosphatase-GFP). The *INP54* gene product from the yeast *Saccharomyces cerevisiae* was selected primarily because its domain structure is compact and appears to contain only a catalytic domain without potential regulatory modules present in other mammalian 5′-phosphatase family members (S. G. et al., unpublished data). Thus, we postulated it would likely function as a constitutively active 5′-phosphatase. In order to determine the substrate selectivity of Inp54p, recombinant protein was produced in bacteria and used to analyze radiolabeled inositol lipid substrates including ^{3}H-PI, -PI(3)P, -PI(4)P, -PI(3,5)P_2, and -PI(4,5)P_2, as well as several D-5 phosphorylated inositol polyphosphates. Mixed bilayer or micellar (inclusion of triton) lipid substrates were incubated with recombinant Inp54p for 30 min, after which reactants were deacylated and the resulting glycerol phosphoinositols (groPIs) were analyzed by HPLC. Comparison of control (top panel) versus enzyme-treated groPIs from micellar substrate reactions shows a depletion of PI(4,5)P_2 and a corresponding increase in the PI(4)P product (Figure 3C). Additionally, recombinant Inp54p under conditions tested thus far, did not show hydrolytic activity toward I(1,4,5)P_3 or Ins(1,3,4,5)P_4 (S. G. and J. D. Y., unpublished data). Thus, our data indicate that Inp54p is selective for 5′ phosphates of lipid substrates and does not utilize soluble inositol polyphosphates involved in Ca^{2+} signaling responses.

We then tested whether the PM-5′-phosphatase-GFP construct hydrolyzes PI(4,5)P_2 in mammalian cells by steady-state labeling of ^{3}H-inositol lipids in COS cells, which can be transfected with high efficiency. A striking decrease in extracted PI(4,5)P_2 lipid (60% reduction) was observed in cells expressing PM-5′-phosphatase-GFP, while the level of PI(3)P was not changed and the level of PI(4)P was only slightly elevated (Figure 3D). The only small elevation of PI(4)P suggests that its concentration is tightly regulated by a PI(4)P hydrolyzing phosphatase.

When the same construct was expressed in NIH-3T3 fibroblasts, adhesion energy was markedly reduced (Figure 3E). As a control, a GFP with a conjugated myristoylation/palmitoylation sequence did not affect adhesion energy (Figure 3E). Together with the reduced adhesion energy in cells expressing the PIP2 sequestering PH domain, this finding strongly supports the hypothesis that PIP2 concentration regulates adhesion energy.

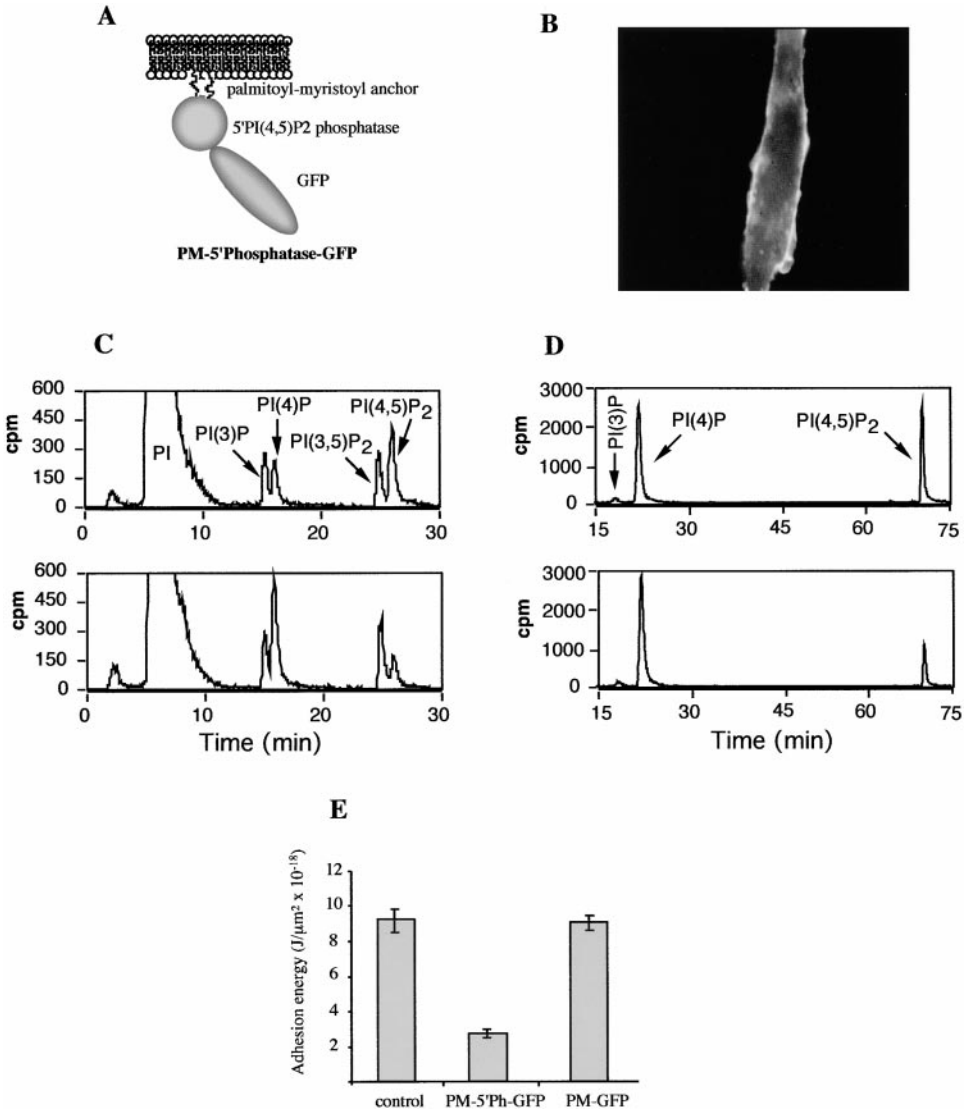

Figure 3. Expression of a Plasma Membrane–Targeted PIP2-Specific 5′-Phosphatase Reduces the Membrane–Cytoskeletal Adhesion Energy

(A) Rational design of a 5′-selective phosphatase fusion protein that is targeted to the plasma membrane in order to reduce the plasma membrane concentration of PIP2.

(B) Plasma membrane localization of the mirystoylated/palmitoylated GFP-5′-phosphatase in NIH-3T3 cells.

(C) PtdIns(4,5)P_2 selectivity of 5′-phosphatase. HPLC radio traces of separated groPIs from control (upper panel) or enzyme (lower panel) treated lipids show more than 3-fold decrease in PI(4,5)P_2, and a corresponding increase in PI(4)P.

(D) Reduction in PIP2 concentration in COS cells transfected with PM-5′-phosphatase-GFP. PI lipids in COS cells were radiolabeled with ^{3}H-inositol and lipids were extracted from control cells and cells expressing PM-5′-phosphatase-GFP. Upper panel, HPLC radio traces of lipids from control cells. Lower panel, HPLC radio traces of lipids from PM-5′-phosphatase-GFP expressing cells.

(E) Expression of PM-5′-phosphatase-GFP induces a marked reduction in adhesion energy while a GFP targeted to the plasma membrane by the same myristoylation/palmitoylation sequence had no effect on adhesion energy.

The expression of the two constructs not only affected adhesion energy but also cell shape. After a period of 5–24 hr required for expression, many of the cells transfected with the GFP-PH(PLCδ) or PM-5′-phosphatase-GFP gained a more rounded appearance, lost their substrate attachment, and often formed membrane blebs (Figure 4A). The measured tether force in both types of blebs was small (Figure 4B), consistent with the previously observed absence of cytoskeletal structures in membrane blebs (Keller and Eggli, 1998; Dai and Sheetz, 1999).

Regulation of Cytoskeletal-Plasma Membrane Adhesion Energy by PIP2 Is Likely Mediated by Actin Polymerization/Depolymerization

How does PIP2 regulate adhesion energy? It is useful to first estimate the number of dynamic binding interactions needed to generate the measured adhesion energy. The calculated adhesion energy density γ of fibroblasts is relatively small ($\sim$9.1 10^{-18} J/μm^2), corresponding to only a few hundred binding interactions per μm^2. This estimate assumes relatively weak and reversible individual binding affinities of $\sim$1 μM with an

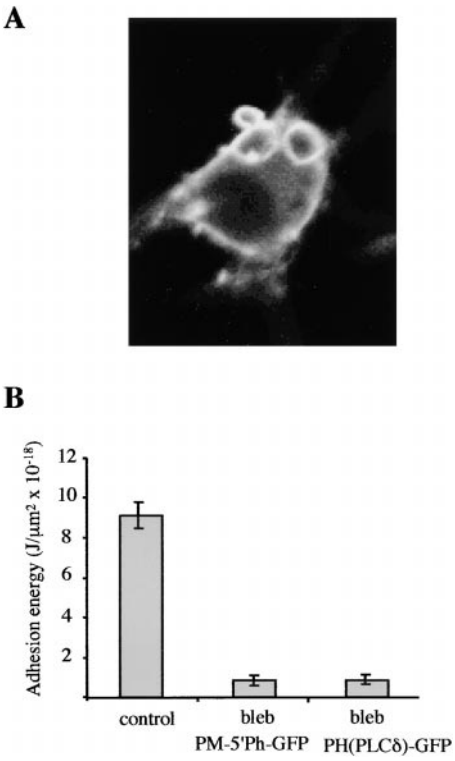

Figure 4. Cell Rounding and Bleb Formation in Cells Expressing GFP-PH(PLCδ) and GFP-5′-Phosphatase

(A) Expression of GFP-PH(PLCδ) often led to a rounding of cells and induced membrane blebs within 5–20 hr of transfection.

(B) Bar diagram of adhesion energies measured in untransfected cells and in blebs of cells transfected with either GFP-PH(PLCδ) or GFP-5′-phosphatase.

average binding energy of $\sim 5 \cdot 10^{-20}$ J per interaction. Since PIP2 lipids have many structural and anchoring functions, it is not surprising that the number of PIP2 lipids in the inner leaflet of the plasma membrane is higher than the number of dynamic binding interactions required to generate adhesion energy. Indeed, if PIP2 is present in a concentration range of 0.1% to 5% of inner plasma membrane bilayer lipids (Kleinig, 1970; Tran et al., 1993), this would correspond to several thousand PIP2 lipids per μm^2. At least in principle, such a higher number of PIP2 molecules compared to the number of dynamic cytoskeletal binding interactions would be consistent with the hypothesis that the PIP2 concentration regulates adhesion energy directly by reducing or adding local binding interactions between the cytoskeleton and the plasma membrane.

However, PIP2 lipids could also regulate adhesion energy indirectly by regulating signaling cascades that alter the cortical cytoskeleton structure. For example gelsolin, which is regulated by PIP2 and calcium, can remodel actin cytoskeleton in response to agonist stimulation (Janmey and Stossel, 1989; Lin et al., 1997). Other PIP2-dependent actin regulators included cofilin, which depolymerizes actin in the absence of PIP2 (Yonezawa et al., 1990). Consistent with an important role for PIP2 in such a signaling pathway, the expression of GFP-5′-phosphatase (Figure 5A, left panel) and of GFP-PH(PLCδ) (Figure 5B, left panel) led to a cell-wide reduction in polymerized F-actin (Figures 5A and 5B, right

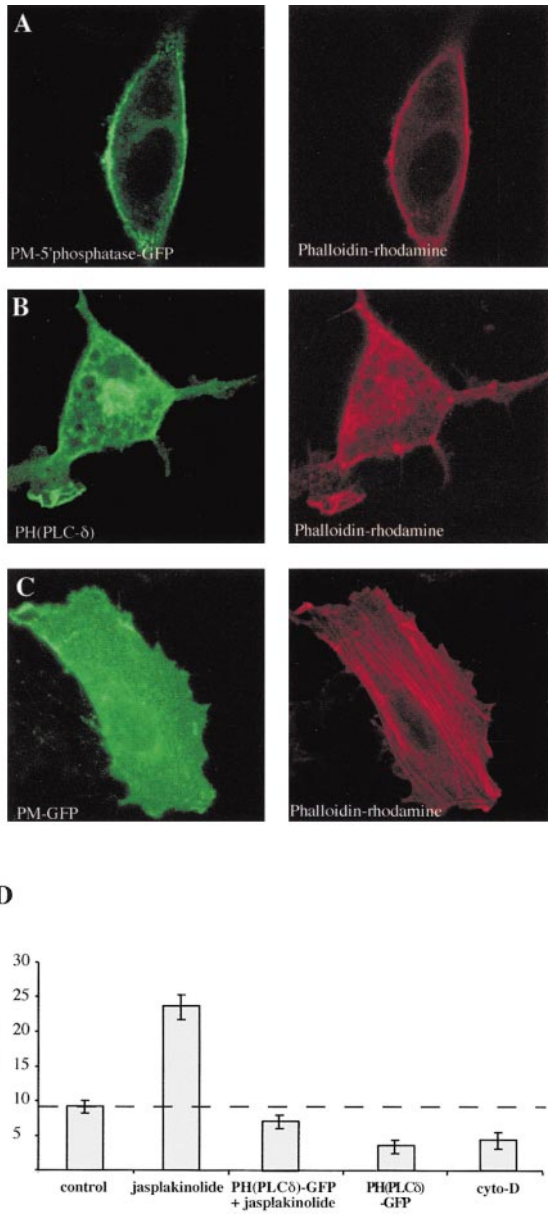

Figure 5. Role of Actin in the Regulation of the Membrane–Cytoskeletal Adhesion Energy

(A) Expression of PM-5′-phosphatase-GFP disrupts polymerized actin in NIH-3T3 cells. Left, fluorescence image of PM-5′-phosphatase GFP. Right, fluorescence image of rhodamine-labeled phalloidin.

(B) Same experiment as in (A) except that GFP-PH(PLCδ) was expressed instead of the PM-5′-phosphatase-GFP.

(C) Control measurements with a plasma membrane–targeted GFP. The plasma membrane staining in (B) and (C) is less apparent than in (A) because flatter fibroblasts are shown.

(D) The actin-polymerizing drug jasplakinolide markedly increases adhesion energy while cytochalasin D, which reduces polymerized actin, reduces adhesion energy. Jasplakinolide also partially reverts the PH domain–induced drop in adhesion energy.

panels). Control cells that expressed a GFP targeted to the plasma membrane by a myristoylation/palmitoylation sequence had intact polymerized actin as can be seen from the intact stress fibers (Figures 5C). Our findings are consistent earlier studies which showed that expressed nontargeted phosphatases or full-length

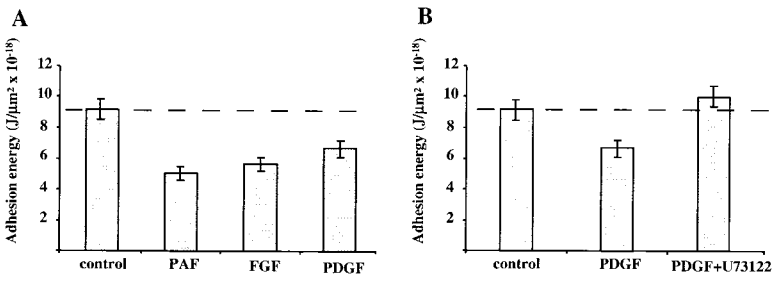

Figure 6. Receptor-Mediated Lowering of Membrane Adhesion Energy

(A) Different receptor stimuli induce a marked reduction in the apparent adhesion energy. Average changes in the adhesion energy in response to 40 ng/ml PDGF, 100 ng/ml PAF and 100 ng/ml EGF activation were measured 10–15 min after receptor stimulation.

(B) Receptor-mediated lowering in adhesion energy is likely mediated by activation of PLC. One micromolar U73122, a PLC inhibitor, reverted the receptor-induced reduction in adhesion energy.

PIP2-binding proteins can disrupt the actin cytoskeleton (Gilmore and Burridge, 1996; Shibasaki et al., 1997).

The important role of actin polymerization and depolymerization in controlling adhesion energy was further supported by the finding that the actin polymerization drug, jasplakinolide (Bubb et al., 1994; Holzinger and Meindl, 1997; Lee et al., 1998) increased the adhesion energy and partially reverted the PH domain–mediated decrease in adhesion energy (Figure 5D). Furthermore, cytochalasin D, which reduces polymerized actin, also reduced adhesion energy. Thus, a main intermediate between changes in PIP2 concentration and adhesion energy is likely an increase and decrease in F-actin cytoskeletal structures. Together, these measurements suggest that PIP2 regulates the local adhesion between cytoskeleton and plasma membrane by regulating F-actin polymerization.

Regulation of Cytoskeletal–Plasma Membrane Adhesion Energy by Signaling Processes that Regulate PIP2 Concentration

Can signal transduction processes directly mediate changes in adhesion energy? We explored the role of receptor-triggered signal transduction in regulating adhesion energy by using stimuli that hydrolyze PIP2 by activating PLCβ (platelet-activating factor [PAF] receptor activation) or stimuli that activate PLCγ (epidermal growth factor [EGF] and platelet-derived activating factor [PDGF] receptors). Figure 6A shows that PAF receptor stimulation of NIH-3T3 cells markedly reduced adhesion energy. Furthermore, adhesion energy was reduced by activation of either EGF or PDGF receptors. This reduction could be blocked by U73122 (Yule and Williams, 1992; Jin et al., 1994; Mogami et al., 1997), an inhibitor of PLC (Figure 6B), suggesting that PLC can be an important player in the control of PIP2 concentration and adhesion energy.

Anchoring and Signaling Roles of PIP2 in Controlling Cytoskeletal–Membrane Adhesion Energy

Together, these measurements lead to a model in which the local adhesion energy is regulated by the local concentration of PIP2 (Figure 7). Receptor stimuli can either increase or decrease local PIP2 concentrations by activating PI(4)P 5′-kinase or by activating PLC, PI3-kinase and 5′-phosphatases, respectively. Local changes in PIP2 concentration can regulate cortical plasma membrane-cytoskeletal structure by directly altering interactions between PIP2 and cytoskeletal anchoring proteins and/or by regulation of actin polymerization via gelsolin, cofilin and other enzymes that increase or decrease actin polymerization. In turn, the polymerization state of cortical actin and the number of binding interactions between PIP2 and cytoskeletal proteins define the local adhesion energy. When the local PIP2 concentration and adhesion energy become small, the swelling pressure within the cell can separate lipid membrane from cytoskeleton and lead to the formation of membrane blebs. This model suggests that changes in cell shape, formation of cell protrusions, endocytosis, cell migration, and other processes can be triggered by increasing and decreasing the local adhesion energy by receptor-controlled changes in local PIP2 concentration.

Experimental Procedures

Cell Culture, Transfection, and Microscopy

NIH-3T3 cells (a mouse fibroblast line) were grown in Dulbecco's modified Eagle medium (DMEM; GIBCO, Grand Island, NY) supple-

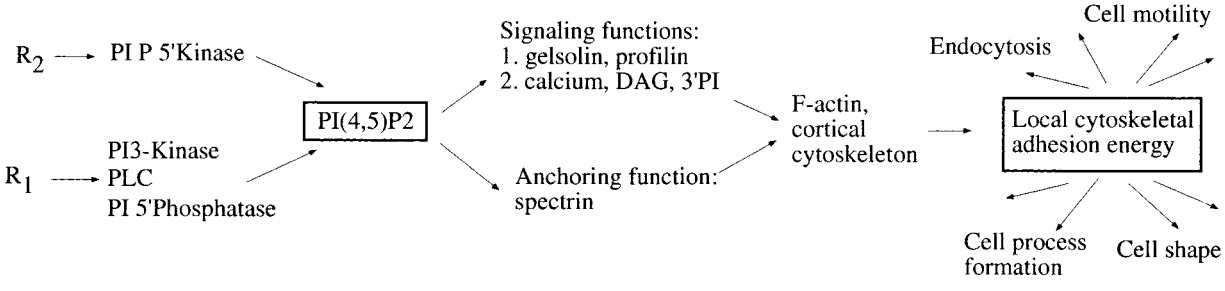

Figure 7. Model for the Role of PIP2 and Adhesion Energy for Different Cell Functions

Different signal transduction processes control plasma membrane PIP2 concentration that in turn regulates the cortical actin cytoskeletal structure and the local adhesion energy. In turn, local adhesion energy controls cell shape, endocytosis, endocytosis, cell movement as well as the formation of cell processes.

mented with 10% fetal bovine serum (GIBCO), 100 units/ml penicillin and 100 mg/ml streptomycin, and 7.5 mM HEPES at 37°C in 5% CO_2. Cells were removed from tissue culture flasks by brief treatment with trypsin-EDTA (GIBCO), and plated onto glass coverslips. Proteins were expressed in NIH-3T3 cells, visualized by confocal laser scanning microscopy (LSM 410, Zeiss, Inc., Thornwood, NY) or by a video-enhanced differential interference contrast (DIC) microscope equipped with laser optical tweezers (Choquet et al., 1997).

For the comparison of GFP expression and actin polymerization, NIH-3T3 cells were cultured on glass coverslips and transfected with GFP fusion construct using LipofectAMINE (Life Technology). Six to ten hours after transfection, the cells were fixed for 10 min at 4°C with 4% paraformaldehyde in PBS, then permeabilized for 5 min at 4°C with 0.1% Triton in PBS. Rhodamine phalloidin (Molecular Probes) was incubated with the cells for 30 min at room temperature at a dilution of 1:600 in PBS.

Labeling of PI Lipids with ^{3}H-Inositol

The lipid compositions of COS cells expressing PM-5′-phosphatase-GFP, or vector alone, were compared. COS cells were plated at 5%–10% confluency in DMEM without inositol and 10% dialyzed FBS. ^{3}H-inositol was added at a final concentration of 10 μCi/ml. The cells were allowed to grow for 3 days at 37°C and 5% CO_2 before transfection. Cells were harvested 24 hr after transfection and cellular lipids were extracted and deacylated. The resultant grolipids were separated by HPLC (two separate experiments showed the same result).

Constructs

The construction of GFP-PH and GFP-PH* from PLCδ was described in Stauffer et al. (1998). GFP-PH from Akt was cloned in to the same SHiro3 vector using PCR reactions. PI(4,5)P_2 specific Inp54p 5′-phosphatase was cloned into SHiro3 vector at the C terminus of GFP. A 10–amino acid peptide was engineered in frame with GFP coding sequence at the N terminus of GFP. The corresponding N-terminal peptide from Lyn is a target for myristoylation and palmitoylation. Subcloned plasmids were transfected either by microporation of RNA or by DNA transfection using LipofectAMINE plus (Life Technology).

Measurement of Adhesion Energy

The tether force was calculated from the displacement of the bead from the center of the laser trap during tether formation using the same calibration protocol of the laser trap described in Dai and Sheetz (1995). The bead was coated with mouse IgG from normal serum (Sigma I-5381) using carbodiimide linkage as described in Kuo and Sheetz (1993).

An equation with the energy terms for lipid tethers pulled from cells was described in Hochmuth et al. (1996). The measured tether force has a bending energy component, a far-field energy component, and an adhesion energy component:

(1) $E(R) = \pi BL/R$ (bending energy of the tether) $+ 2\pi RTL$ (far-field tension term) $+ 2\pi R\gamma L$ (loss of adhesion energy),

with B as the bilayer bending module, L as the length of the tether, R as the tether radius, γ as the cytoskeletal to plasma membrane adhesion energy density, and T as the far-field tension. This equation is based on the observation that tethers do not contain cytoskeletal structures. The energy representation is more clear than the force or tension representation since the different terms that contribute to the description of tethers are additive.

The far-field tension term in nonspherical cells with a strong membrane cytoskeletal interaction is small in comparison to the adhesion term and can therefore be dropped from equation (1):

(2) $E(R) = \pi BL/R + 2\pi R\gamma L$.

The energy equation (2) reaches its minimum for:

(3) $dE/dR = 0$ or $R = [B/2\gamma]^{1/2}$.

This results in a relationship between the tether force (F) and the membrane adhesion energy (γ) that is independent of R and L:

(4) $F = dE/dL = 2\pi[2\gamma B]^{1/2}$ or

(5) $\gamma = F^2/[8\pi^2 B]$.

The latter expression for γ was used in our study to calculate the adhesion energy from the measured tether force.

The fibroblast bilayer bending modulus, $B = 6.8\ 10^{-20}$ J, was estimated by measuring a tether diameter of ~0.34 μm and a force of 2.5 pN in blebs of NIH-3T3 fibroblasts using a relationship previously derived (Waugh and Hochmuth, 1987):

(6) $B = F \cdot R/[2\pi]$.

Fibroblasts with blebs were used for these studies, since the diameters of tethers pulled from blebs were large enough to be measured by light microscopy.

Acknowledgments

This work supported by National Institutes of Health grants GM 48113 to T. M., GM 362277 to M. P. S., and HL 55672 to J. D. Y.

Received September 9, 1999; revised December 21, 1999.

References

Berk, D.A., and Hochmuth, R.M. (1992). Lateral mobility of integral proteins in red blood cell tethers. Biophys. J. *61*, 9–18.

Bubb, M.R., Senderowicz, A.M., Sausville, E.A., Duncan, K.L., and Korn, E.D. (1994). Jasplakinolide, a cytotoxic natural product, induces actin polymerization and competitively inhibits the binding of phalloidin to F-actin. J. Biol. Chem. *269*, 14869–14871.

Choquet, D., Felsenfeld, D.P., and Sheetz, M.P. (1997). Extracellular matrix rigidity causes strengthening of integrin-cytoskeleton linkages. Cell *88*, 39–48.

Dai, J., and Sheetz, M.P. (1995). Mechanical properties of neuronal growth cone membranes studied by tether formation with laser optical tweezers. Biophys. J. *68*, 988–996.

Dai, J., and Sheetz, M.P. (1999). Membrane tether formation from blebbing cells. Biophys. J., in press.

Franke, T.F., Kaplan, D.R., Cantley, L.C., and Toker, A. (1997). Direct regulation of the Akt proto-oncogene product by phosphatidylinositol-3,4-bisphosphate. Science *275*, 665–668.

Gilmore, A.P., and Burridge, K. (1996). Regulation of vinculin binding to talin and actin by phosphatidyl-inositol-4-5-bisphosphate. Nature *381*, 531–535.

Hochmuth, F.M., Shao, J.Y., Dai, J., and Sheetz, M.P. (1996). Deformation and flow of membrane into tethers extracted from neuronal growth cones. Biophys. J. *70*, 358–369.

Holzinger, A., and Meindl, U. (1997). Jasplakinolide, a novel actin targeting peptide, inhibits cell growth and induces actin filament polymerization in the green alga Micrasterias. Cell Motil. Cytoskeleton *38*, 365–372.

Isakoff, S.J., Cardozo, T., Andreev, J., Li, Z., Ferguson, K.M., Abagyan, R., Lemmon, M.A., Aronheim, A., and Skolnik, E.Y. (1998). Identification and analysis of PH domain–containing targets of phosphatidylinositol 3-kinase using a novel in vivo assay in yeast. EMBO J. *17*, 5374–5387.

Janmey, P.A. (1995). Protein regulation by phosphatidylinositol lipids. Chem. Biol. *2*, 61–65.

Janmey, P.A., and Stossel, T.P. (1989). Gelsolin-polyphosphoinositide interaction. Full expression of gelsolin-inhibiting function by polyphosphoinositides in vesicular form and inactivation by dilution, aggregation, or masking of the inositol head group. J. Biol. Chem. *264*, 4825–4831.

Jin, W., Lo, T.M., Loh, H.H., and Thayer, S.A. (1994). U73122 inhibits phospholipase C–dependent calcium mobilization in neuronal cells. Brain. Res. *642*, 237–243.

Kandzari, D.E., Chen, J., and Goldschmidt-Clermont, P.J. (1996). Regulation of the actin cytoskeleton by inositol phospholipid pathways. Subcell. Biochem. *26*, 97–114.

Keller, H., and Eggli, P. (1998). Protrusive activity, cytoplasmic compartmentalization, and restriction rings in locomoting blebbing Walker carcinosarcoma cells are related to detachment of cortical ac193. Cell Motil. Cytoskeleton *41*, 181–193.

Kleinig, H. (1970). Nuclear membranes from mammalian liver. II. Lipid composition. J. Cell Biol. *46*, 396–402.

Kuo, S.C., and Sheetz, M.P. (1993). Force of single kinesin molecules measured with optical tweezers. Science *60*, 232–234.

Lee, E., Shelden, E.A., and Knecht, D.A. (1998). Formation of F-actin aggregates in cells treated with actin stabilizing drugs. Cell Motil. Cytoskeleton *39*, 122–133.

Lin, K.M., Wenegieme, E., Lu, P.J., Chen, C.S., and Yin, H.L. (1997). Gelsolin binding to phosphatidylinositol 4,5-bisphosphate is modulated by calcium and pH. J. Biol. Chem. *272*, 20443–20450.

Mogami, H., Lloyd Mills, C., and Gallacher, D.V. (1997). Phospholipase C inhibitor, U73122, releases intracellular Ca^{2+}, potentiates $Ins(1,4,5)P_3$-mediated Ca^{2+} release and directly activates ion channels in mouse pancreatic acinar cells. Biochem. J. *324*, 645–651.

Raucher, D., and Sheetz, M.P. (1999). Membrane expansion increases endocytosis rate during mitosis. J. Cell Biol. *144*, 497–506.

Ren, X.D., and Schwartz, M.A. (1998). Regulation of inositol lipid kinases by Rho and Rac. Curr. Opin. Genet. Dev. *8*, 63–67.

Shibasaki, Y., Ishihara, H., Kizuki, N., Asano, T., Oka, Y., and Yazaki, Y. (1997). Massive actin polymerization induced by phosphatidylinositol-4-phosphate 5-kinase in vivo. J. Biol. Chem. *272*, 7578–7581.

Stauffer, T.P., Ahn, S., and Meyer, T. (1998). Receptor-induced transient reduction in plasma membrane $PtdIns(4,5)P_2$ concentration monitored in living cells. Curr. Biol. *8*, 343–346.

Stolz, L.E., Kuo, W.J., Longchamps, J., Sekhon, M.K., and York, J.D. (1998). INP51, a yeast inositol polyphosphate 5-phosphatase required for phosphatidylinositol 4,5-bisphosphate homeostasis and whose absence confers a cold-resistant phenotype. J. Biol. Chem. *273*, 11852–11861.

Tran, D., Gascard, P., Berthon, B., Fukami, K., Takenawa, T., Giraud, F., and Claret, M. (1993). Cellular distribution of polyphosphoinositides in rat hepatocytes. Cell Signal. *5*, 565–581.

Waugh, R.E., and Bauserman, R.G. (1995). Physical measurements of bilayer-skeletal separation forces. Ann. Biomed. Eng. *23*, 308–321.

Waugh, R.E., and Hochmuth, R.M. (1987). Mechanical equilibrium of thick, hollow, liquid membrane cylinders. Biophys. J. *52*, 391–400.

Yonezawa, N., Nishida, E., Iida, K., Yahara, I., and Sakai, H. (1990). Inhibition of the interactions of cofilin, destrin, and deoxyribonuclease I with actin by phosphoinositides. J. Biol. Chem. *265*, 8382–8386.

Yule, D.I., and Williams, J.A. (1992). U73122 inhibits Ca^{2+} oscillations in response to cholecystokinin and carbachol but not to JMV-180 in rat pancreatic acinar cells. J. Biol. Chem. *267*, 13830–13835.